Applied Thermal Engineering 73 (2014) 931–939

Contents lists available at ScienceDirect

Applied Thermal Engineering

journal homepage: www.elsevier.com/locate/apthermeng

Analysis of a new methodology applied to the desorption of natural gas in activated carbon vessels

J.C. Santos [a], J.M. Gurgel [b], F. Marcondes [c, *]

[a] Department of Mechanical Production Engineering, Regional University of Cariri, Av. Leão Sampaio, S/N, Juazeiro do Norte, Ceará 63040-000, Brazil
[b] Department of Mechanical Engineering, Federal University of Paraiba, LES/UFPB – Cidade Universitária, João Pessoa, Paraíba 58090-900, Brazil
[c] Department of Metallurgical Engineering and Material Science, Federal University of Ceará, Campus do Pici, Bloco 714, Fortaleza, Ceará 60455-760, Brazil

HIGHLIGHTS

- The desorption of natural gas in activated carbon is investigated.
- A 1D model based on mass and energy for pellets and column is investigated.
- A numerical code was developed to analyze the dynamics of discharge.
- The effect of regeneration temperature and pressure drop on desorption process is investigated.

ARTICLE INFO

Article history:
Received 13 February 2014
Accepted 21 August 2014
Available online 30 August 2014

Keywords:
Adsorbed natural gas
Discharge process
Activated carbon
Finite-volume method

ABSTRACT

The presented work performs a numerical investigation of natural gas desorption process in activated carbon vessels. The numerical results show that increasing the inlet temperature of gas increases the desorption of the adsorbed material. It also observed that the desorption time is a function of the applied pressure drop. For the investigated cases of the presented work, the desorption time varied from 250 s to 600 s. It is proposed that in order to reduce the negative effects of the heat of adsorption to the process, one fraction of desorbed gas must be circulated in an external heat exchange to use the energy of exhaustion gas to increase the gas's inlet temperature. This approach avoids the use of additional devices to the system, such as external heating jackets and fins that increase the complexity of the system.

1. Introduction

Today, one of the main concerns of environmentalists and researchers is related to the gas emissions that cause the greenhouse effect in the atmosphere, especially that caused by carbon dioxide. Emissions of carbon dioxide in the atmosphere result mainly from burning fossil fuels and deforestation. Natural gas (NG) is an excellent alternative fuel for application in automotive vehicles since it is cheaper than gas and diesel and produces a cleaner combustion with less carbon dioxide and other air pollutant emissions. Without major engineering drawbacks, the actual automotive engines can be converted to using NG. However, the drawbacks associated to the storage and transportation has limited the large-scale use of NG. NG mainly consists of about 95% methane, which in turn cannot be liquefied at ambient temperature. Therefore, the storage of NG requires the use of expensive high pressure compression process (about 20 MPa) [1]. Additionally, the vases of compressed natural gas (CNG) reduce the available space in automotive vehicles, and due to weight, require the suspension to be reinforced. Therefore, in order to use safe and light tanks and to reduce the compression costs, all efforts have been addressed to reduce the storage pressure. Also, working in reduced pressure allows different geometries to be employed rather than cylindrical tubes, and thus provides a greater design flexibility. Finally, if the pressure is reduced, it is possible to use lighter material such as aluminum.

A storage system by adsorption is one viable technology choice to lower the pressure storage (3.5–4 MPa) of NG, which represents a good compromise between compression costs and storage capacity [2]. The adsorbed natural gas (ANG) is based on high-density gas confined within the adsorbent's pores that offsets the volume taken by the media's solid particles and the low density of the compressed gas that resides in the voids between the adsorbent particles [3]. Currently, microporous-activated carbons have presented the best performance in conjunction with NG vessels. However, there are two drawbacks in the ANG systems that are not

* Corresponding author. Tel.: +55 85 3366 9355; fax: +55 85 3366 9969.
E-mail address: marcondes@ufc.br (F. Marcondes).

http://dx.doi.org/10.1016/j.applthermaleng.2014.08.046
1359-4311/

found in the CNG systems. The first is related to the shape of the adsorption isotherm (type I isotherm), which avoids a linear response of the system relative to the pressure. The second problem is related to the dependence between the adsorption equilibrium and the adsorbent temperature. While the physical adsorption of a gas is an exothermic phenomenon, the gas desorption is endothermic. During the fast charge of the ANG system, in conditions in which the heat of adsorption is not removed, less methane is adsorbed into the system when the temperature increases. Alternatively, during the discharge cycle, the temperature decreases; therefore less gas is released to the corresponding discharge pressure. Ridha et al. [4] and Ridha et al. al [5] showed the harmful effects associated with the heat of adsorption in ANG vessels.

In order to minimize the effects of heat of adsorption in ANG vessels, various solutions have been proposed [3,6–8]. All of these solutions require accessories to be inserted into the tank which, reduce the space available for gas storing, increase the complexity of the project, and have serious limitations in the heat transfer process due to the low effective thermal conductivity of the activated carbon bed. The main problem of the aforementioned solutions is that all heat generated in the adsorbent bed is dissipated by conduction only.

A new tank configuration was proposed by Santos et al. [9] to analyze the charge process in ANG vessels using the constant velocity assumption in the numerical model. In this work, we neglect the assumption of constant velocity to investigate the dynamics of the desorption of natural gas in activated carbon. The effect of regeneration temperature and pressure drop applied in the gas desorption process performance is analyzed. Based on the numerical results, a new methodology for discharging natural gas in activated carbon vessels is proposed. The new vessel consists of several tubes packed with activated carbon; the new system uses forced convection between the adsorbent and the gas flow in order to increase the rate of heat transfer in the adsorbent bed.

2. Mathematical model

Fig. 1 shows the configuration investigated. In order to perform the analysis, a single column filled up with activated carbon and open on both sides is considered. The natural gas flows from one side of the column to the other. The constitutive equations are based on the mass, momentum and energy balances [10,11] and ideal gas equation. Next, we show the models along with the initial and boundary conditions for the column and the adsorbent material.

2.1. Column model

For the column model, the following assumptions are considered:

- Radial effects are neglected;
- The natural gas is constituted of pure methane;
- The sorbate behaves as ideal gas.

Under the above assumptions, the column model is constituted by the continuity equation, momentum equation, energy equation, and the perfect gas equation, respectively:

$$\frac{\partial \rho_f}{\partial t} + \frac{\partial}{\partial x}(\rho_f u) = -\frac{1-\varepsilon}{\varepsilon}\frac{\partial \overline{q}}{\partial t} \tag{1}$$

$$\frac{\partial}{\partial t}(\rho_f u) + \frac{\partial}{\partial x}(\rho_f uu) = -\frac{\partial p}{\partial x} - \frac{150\mu}{d_p^2}\frac{(1-\varepsilon)^2 u}{\varepsilon^2} - \frac{1.75\rho_f}{d_p}\frac{(1-\varepsilon)u^2}{\varepsilon} \tag{2}$$

$$\frac{\partial}{\partial t}(\rho_f T_f) + \frac{\partial}{\partial x}(\rho_f u T_f) = \frac{\partial}{\partial x}\left(\frac{\lambda_f}{cp_f}\frac{\partial T_f}{\partial x}\right) + \frac{6h_p}{d_p}\frac{(1-\varepsilon)}{\varepsilon cp_f}\left(T_s - T_f\right) + \frac{2U_g(T_\infty - T_f)}{\varepsilon R_i cp_f} \tag{3}$$

$$\rho_f = \frac{p}{R_g T_f} \tag{4}$$

where ρ_f is the density of gas (kg/m^3), p is the pressure (Pa), T is the temperature (K), λ is the thermal conductivity (W/m K), ε is the bed porosity, R_g is the ideal gas constant (J/kg K), c_p is the specific heat at constant pressure (J/kg K), d_p is the pellet diameter (m), U_g is the overall heat transfer coefficient (W/m^2 K), R_i is the internal column radius (m), and subscript f denotes the fluid phase.

In order to study the desorption process, it is assumed that an overheated gas stream with constant temperature (T_{in}) and pressure (p_{in}) is suddenly forced into an activated carbon packed column which is initially saturated with gas at a temperature (T_0) and pressure (p_0). The outlet pressure is kept at $p_{0,}$ while the initial temperature is assumed to be equal to ambient temperature. Therefore, the bed equations are subjected to the following initial and boundary conditions:

$$p(x, t=0) = p_0; \quad T_f(x, t=0) = T_0; \quad u(x, t=0) = u_0 \tag{5}$$

$$p(x=0, t) = p_{in}; \quad T_f(x=0, t) = T_{in} \tag{6}$$

$$p(x=L, t) = p_0; \quad \frac{\partial T_f(x=L, t)}{\partial x} = 0 \tag{7}$$

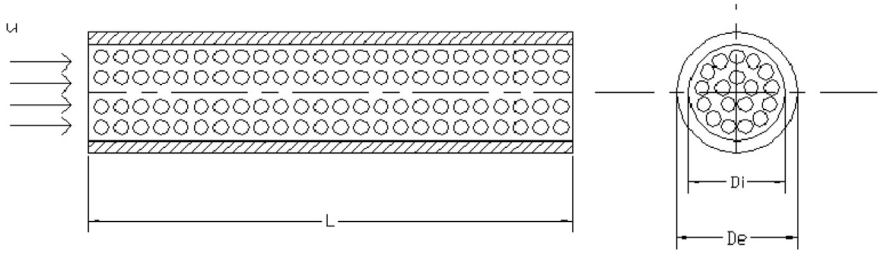

Fig. 1. Activated carbon packed column.

2.2. Pellet model

The following assumptions are applied to the pellets:

- Pellets are considered as spherical particles and uniformly distributed;
- The monodisperse model is used to describe the adsorption kinetics in the adsorbent, and the effective mass diffusion coefficient is considered constant;
- Temperature is uniform inside the adsorbent particles;
- Adsorption equilibrium is assumed in the external surface of the adsorbent particles.

Using the above assumptions, the mass and energy balance equations to the pellet are, respectively, given by:

$$\frac{\partial q}{\partial t} = \frac{1}{r^2}\frac{\partial}{\partial r}\left(r^2 D_{ef}\frac{\partial q}{\partial r}\right) \tag{8}$$

$$C_s\frac{\partial T_s}{\partial t} = \frac{6h_P}{d_P}(T_f - T_S) + (-\Delta H)\frac{\partial \overline{q}}{\partial t} \tag{9}$$

where q denotes the concentration of gas in the solid phase (kg/m^3), r is the radius (m), D_{ef} is the effective mass diffusion coefficient (m^2/s), ΔH is the heat of adsorption (J/kg), $\overline{q}$ is the volumetric average concentration of the gas in the adsorbent particle (kg/m^3), h_p is the convection heat transfer coefficient in pellet surface (W/m^2 K), and the subscript S denotes the solid phase.

The initial and boundary conditions to the pellet equations are given by:

$$q(r, t=0) = q^*(p_0, T_0); \quad T_S(t=0) = T_0 \tag{10}$$

$$\frac{\partial q(r=0,t)}{\partial r} = 0 \tag{11}$$

$$q(r = R_P, t) = q^*(p, T_S) \tag{12}$$

2.3. Determination of the heat transfer coefficients

The fluid-particle heat transfer coefficient h_p is given by the following correlation described in Ruthven [10]:

$$Nu_p = \frac{h_p d_p}{\lambda_f} = 2 + 1.1 Pr^{1/3} Re^{0.6} \tag{13}$$

The overall heat transfer resistance in the column wall is given by the sum of the inner convective resistance, wall conductive resistance, and outer convective resistance. Therefore, the overall heat transfer coefficient U_g is given by:

$$U_g = \frac{1}{\frac{1}{h_i} + \frac{R_i}{\lambda_w}\ln\left(\frac{R_e}{R_i}\right) + \frac{R_i}{R_e}\frac{1}{h_e}} \tag{14}$$

The inner convective coefficient is given by Ruthven [10]:

$$Nu_i = \frac{h_i D_i}{\lambda_f} = 0.813 Re^{0.19}\exp(-6d_p/D_i) \tag{15}$$

To evaluate the external convective coefficient, forced convection conditions were assumed. The external convective coefficient is given by the following correlation described in Incropera and DeWitt [12]:

$$Nu_e = \frac{h_e D_e}{\lambda_{air}} = 0.193 Re^{0.618} Pr^{1/3} \tag{16}$$

3. Numerical procedure

The equations for the column model and the mass balance equation for the pellet are solved by the finite-volume method [13,14]. The pressure–velocity coupling was treated by the PRIME (Implicit Pressure Explicit Momentum) method [15], while the staggered arrangement was used to storage the variables in the computational grid. The WUDS (Weight Upwind Differencing Scheme) by Raithby and Torrance [16] is used to evaluate the physical properties in the interfaces of each control volume. In each time-step, an iterative procedure is performed in order to treat the non-linearities and coupling between equations. The linear systems are solved by the tri-diagonal matrix algorithm. In order to evaluate the velocities in the inlet and outlet of the column, we used the procedure suggested by Marcondes and Maliska [17], while the gas temperature is obtained by the energy equation and the gas density by the ideal law gas. For the pellets, the mass and energy balances are used to determine the volumetric average concentration and temperature, respectively. It is important to mention that the last two variables are the source terms to the column model, in the mass and energy balances, respectively. For the column and pellets, it was used 100 and 10 volumes, respectively. Grid refinement study was performed, but the results did not change when more refined grids were used. Finally, it is important to mention that all simulations were performed using a constant time-step equal to 5×10^{-4} s. The iterative procedure to obtain the solution in each time-step involves the following steps:

1) To supply the initial values of the variables p, u, T_f, q, and T_S.
2) To solve Equation (8) in each control volume of the column and obtain the concentration field of sorbent.
3) To solve Equation (9) in each control volume of the column and obtain the temperature inside each pellet.
4) To calculate the pressure field through continuity Equation.
5) To calculate the velocity field through momentum Equation.
6) To calculate the temperature field through energy Equation.
7) To calculate the density field through perfect gas equation.
8) To return to step 2 and iterate until convergence is reached at the current time level.
9) To progress to the next time level.

To check the solution, in each time-step, the following convergence criteria was used:

$$\left|\frac{\phi_P^{k+1} - \phi_P^k}{\phi_{max} - \phi_{min}}\right| \leq 10^{-5} \tag{17}$$

Here, $|\phi_{max} - \phi_{min}|$ represents the maximum variation of the gas density at k-th iteration. When Eq. (17) is not satisfied, for each control volume, an additional iteration is required.

4. Numerical validation

There is not much experimental data available in the literature regarding the desorption of methane in activated carbon. Most works present only the results in terms of adsorption equilibrium, or simply show only the experiment data for the adsorption but do not report the data for desorption process. Malek and Farooq [18] conducted a very detailed investigation about the adsorption and desorption processes of diluted methane in activated carbon. In their work, experimental data for the breakthrough curves of

methane, ethane, and propane in activated carbon and silica gel were determined for three temperatures (299.15, 318.15, 338.15 K), two particle sizes (0.129, 0.258 cm), several gas velocities (1.3–4.3 cm/s), and various feed pressures (1.99–6.41 bar). The helium was used as a carrier gas in the diluted mixture. The authors developed a mathematical model to analyze the experimental breakthrough curves. The adsorption equilibrium was described by the Langmuir–Freundlich isotherm, while a linear driving force model (LDF) was used to describe the kinetics of adsorption in the adsorbent. From the adjustment between the experimental and numerical data, the authors determined the overall mass transfer coefficient of the adsorbent and the heat transfer coefficient between the adsorbent and the wall of the column. Essentially, the experimental apparatus consisted of a column packed with adsorbent, a concentration detector, and some control devices. In order to allow an isothermal process, the adsorbent column was surrounded by an outer jacket that was circulated by water. Three thermocouples were placed in the bed for measuring the temperature profiles: inlet, middle, and outlet of the column. A flow controller and a pressure regulator were used to control the gas flow rate and the pressure at the inlet of the column, respectively. The adsorbed concentration at the outlet of the column was recorded by a thermal conductivity detector (TCD). A bed free of any trace of methane and helium (carrier gas) was used for the adsorption experiments, while for the desorption experiments, a saturated bed was regenerated using pure helium flow in the column. Identical conditions of pressure, temperature, and velocity were used in the adsorption and regeneration tests of the bed.

Since the main scope of this work is the investigation of the dynamics of desorption of methane in activated carbon, we selected case study 3 from the work of Malek and Farooq [18] for the numerical validation of our approach. Case study 3 presents the breakthrough curves for the adsorption and desorption of methane in activated carbon. The results for a mixture of methane (5%) and helium (95%) in terms of breakthrough curves for desorption and adsorption processes are shown in Fig. 2 of [18]. The following pressure, temperature, and velocity were used in the experiment: 2.4848 bar, 299.15 K, and 1.56 cm/s. A stainless steel column with an internal diameter of 3.5 cm and a length of 40 cm were used in the adsorption and desorption tests. In order to simulate the experiment conducted by Malek and Farooq [18], we added an equation similar to Eq. (1) for the methane plus helium mixture. Fig. 2 shows a comparison of the breakthrough curves obtained in this work with the experimental results of [18] for the adsorption and desorption of methane in activated carbon. The best adjustment between the experimental and numerical results was obtained when the effective mass diffusion coefficient was set to 10×10^{-3} cm^2/s. This value is of the same order of magnitude as the diffusion coefficient determined by Malek and Farooq [18], which was equal to 9.41×10^{-3} cm^2/s Fig. 3 shows a comparison of the temperature profiles obtained in the present work with the experimental profiles from Malek and Farooq [18] at the mid-point and outlet of the column for the adsorption test. The heat transfer coefficient between the adsorbent and the column wall was set to 25 W/(m^2 K). From the results present in Figs. 2 and 3, we can observe a good agreement between the numerical results obtained in this work and the experimental data from Ref. [18]. Therefore, we are going to assume that the computational code developed satisfactorily represents the dynamics of adsorption and desorption of methane in activated carbon.

5. Results and discussions

The geometrical dimensions of the column and other data used in the simulations presented in this section are shown in Table 1.

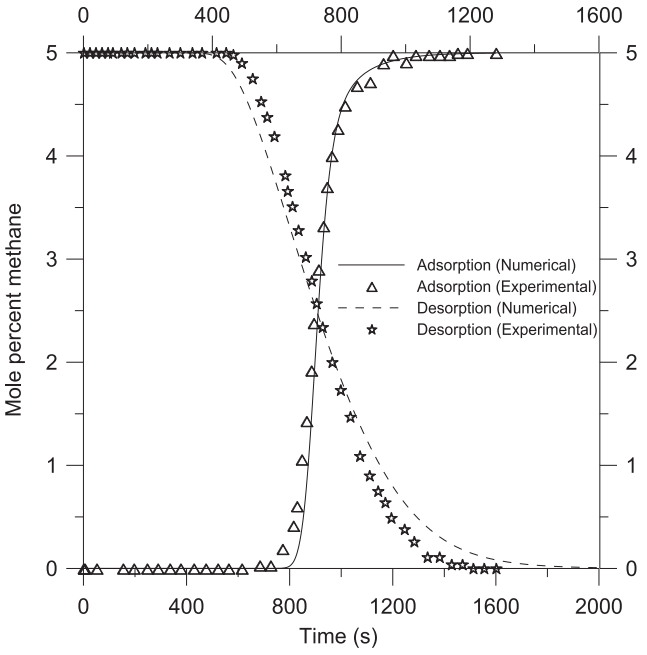

Fig. 2. Comparison of experimental and simulated breakthrough curve.

The packed adsorbent used in the column is G216 of North American Carbon coal Inc., of Columbus, Ohio. The adsorption equilibrium is given by the Langmuir isotherm. The fitting parameters of the isotherm were obtained from experimental data published by Remick and Tiller [19].

$$q^*(p, T_s) = \frac{q_m b p}{1 + bp}, \tag{18}$$

with

$$q_m = 55920 T_s^{-2.3} \tag{19}$$

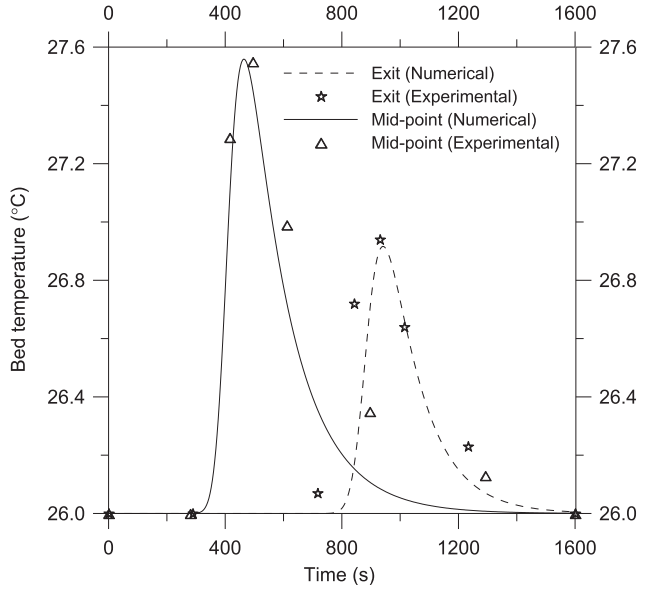

Fig. 3. Comparison of experimental and simulated temperature profiles.

Table 1
Data and physical properties used in the simulations.

Particle radius, R_p	0.5 mm
Column length, L	0.5 m
Column inner radius, R_i	2.5 cm
Initial pressure, p_0	3.5 MPa
Initial temperature, T_0	300.3 K
Pressure drop, $d_p = p_{in} - p_{out}$	400, 700, 1000, 1300 Pa
Inlet temperature, T_{in}	100, 200, 300, 400 °C
Mass diffusion coefficient, D_{ef}	2.5×10^{-8} m^2/s, Cess [20]
Ideal gas constant, R_g	518.35 J/kg K
Bed porosity, ε	0.4
Adsorbent density, ρ_s	2150 kg/m^3, Mota [1]
Adsorbent specific heat, C_{ps}	648 J/kg K, Mota [1]
Effective thermal conductivity of the bed, λ_{ef}	0.2 W/m K, Mota [3]
Sorbate specific heat, C_{pg}	2450 J/kg K, Mota [1]
Surrounding temperature, T_∞	300.3 K
Adsorption heat, ΔH	-1.1×10^6 J/kg, Mota [1]
Wall thickness	0.4 cm
Wall thermal conductivity	15.1 W/m K

$$b = 1.0863 \times 10^{-7} \exp(806/T_s) \quad (20)$$

Activated charcoal has high diffusion time constant, $D_{ef}/R_p^2 \cong 10^{-1}$ s^{-1} [20], for the adsorption of methane. Consequently, activated carbons typically provide low resistance to the mass diffusion. Fig. 4 shows the velocity profiles for an imposed pressure drop equal to 700 Pa. From the profiles, we can observe a sharp reduction of the gas velocity in the region where the mass transfer occurs. However, before and after this region the gas velocity remains constant. Therefore, we can see that the desorption process has a large impact in the gas velocity. After 500 s, when the desorption process is completed, the gas velocity is constant for the whole column. Fig. 5 presents the effect of the desorption process in the pressure profiles. Initially before the desorption starts, the pressure gradient is almost constant for the whole column. However, after the desorption evolves through the column, the pressure profile can be decomposed in two linear curves. The change in the curve inclination is again affected by mass transfer. Finally, after 500 s a constant pressure gradient is observed for the whole column denoting that the desorption process has finished. Fig. 6 shows

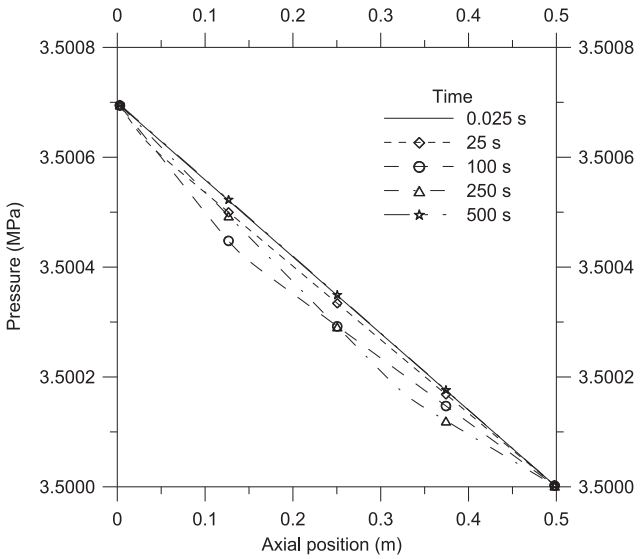

Fig. 5. Axial pressure profiles.

temperature profiles versus time, obtained in five different points of the adsorbent bed. The inlet gas temperature is equal to 400 °C. The curves are shown according to their axial position in the column. For nx volumes used in the simulation, the volume [1] corresponds to the first volume of the computational mesh and volume [nx] refers to the last volume. In Fig. 6, it is observed that the temperature at each point of the column increases until a condition of equilibrium with the flowing gas is reached. It is also observed that about 500 s are required for the entire column to reach thermal equilibrium with the injected gas.

Fig. 7 shows the desorbed mass profiles in the adsorbent bed. Due to the dependence of the adsorption equilibrium with the temperature, it is observed as an inverse behavior of the temperature profiles presented in Fig. 6. At the points at which the bed reaches its maximum temperature, the minimum value for the adsorbed mass is also reached. This value is different from zero

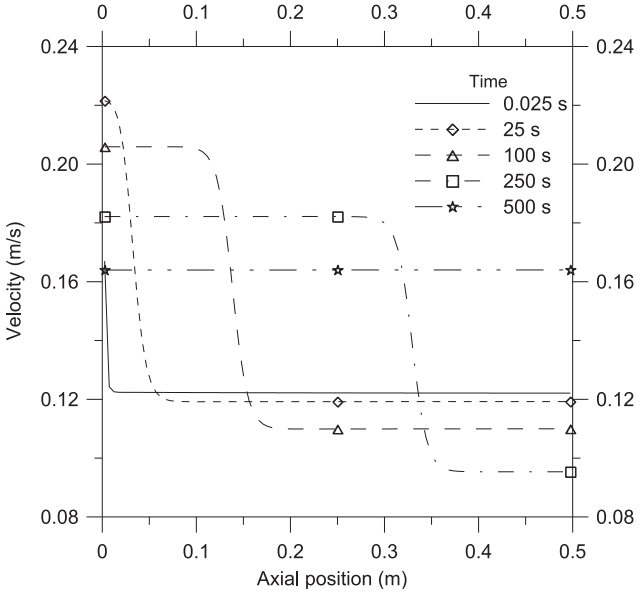

Fig. 4. Axial velocity profiles.

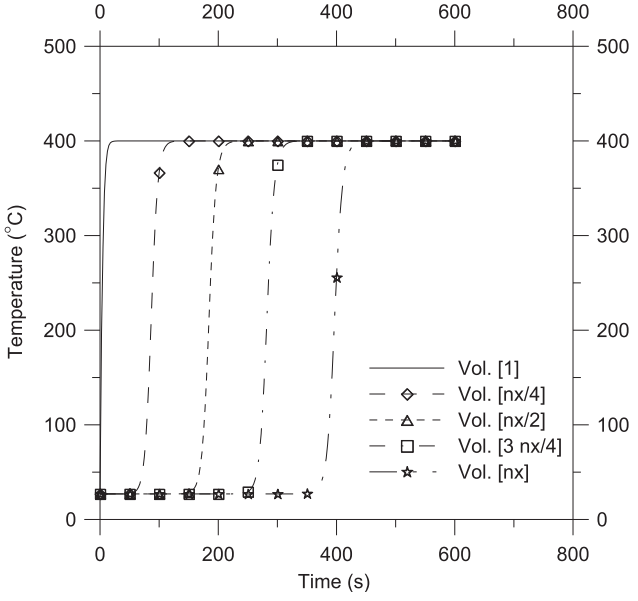

Fig. 6. Temperature profiles.

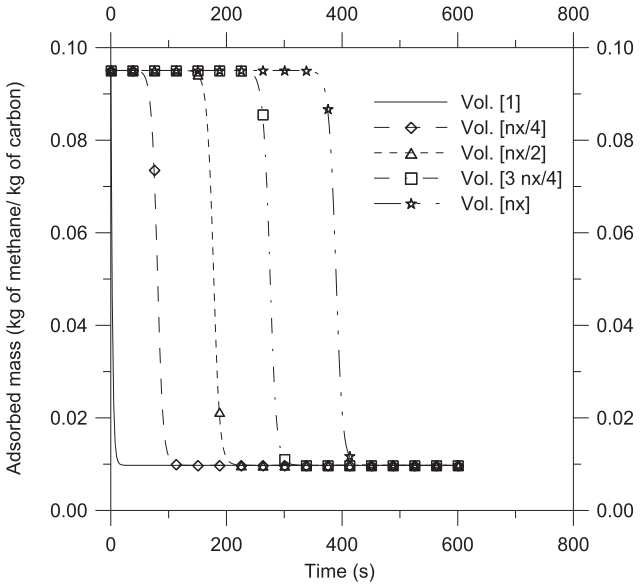

Fig. 7. Profiles of adsorbed mass.

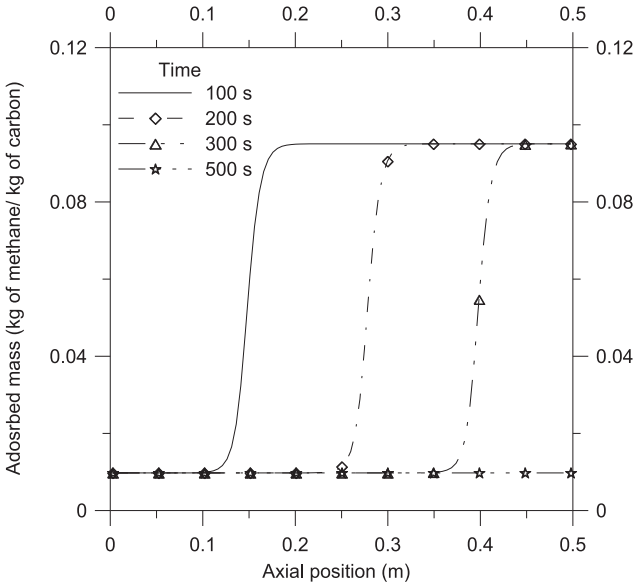

Fig. 9. Evolution of the desorption front into the column.

since it is not practical to operate the column below atmospheric pressure, and it would also not be feasible to use high temperatures to regenerate the column. It is also observed that about 500 s are required for the column to reach its minimum adsorbed mass.

Fig. 8 shows the temperature front in the column, while Fig. 9 presents the desorption front. Insofar as the hot regeneration gas moves in the column, the adsorbed mass profiles decay to its minimum value due to desorption of gas.

5.1. Influence of the regeneration temperature in the performance of desorption process

Now, the influence of the regeneration temperature to the desorption of natural gas in activated carbon is investigated. Four values of the regeneration temperature are analyzed: 100, 200, 300, and 400 °C. Fig. 10 shows the evolution of the average temperature of the adsorbent bed versus time for the four regeneration temperatures studied. It is observed that the average bed temperature increases linearly until reaching the employed corresponding regeneration temperature. It was also observed that the higher the employed regeneration temperature, the higher the average temperature in the adsorbent bed. Fig. 11 shows the effect of regeneration temperature in the desorbed mass. From this figure, it is possible to observe that the use of higher temperature regeneration implies a smaller amount of adsorbed gas into the column by the end of the discharge process. However, it can also be observed in Fig. 11 that the progressive increase in regeneration temperature above 300 °C does not promote a substantial reduction in the adsorbed mass.

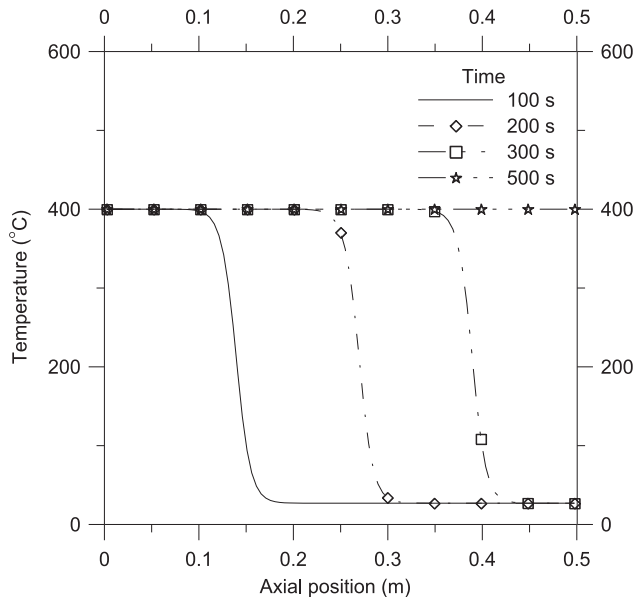

Fig. 8. Evolution of the temperature front into the column.

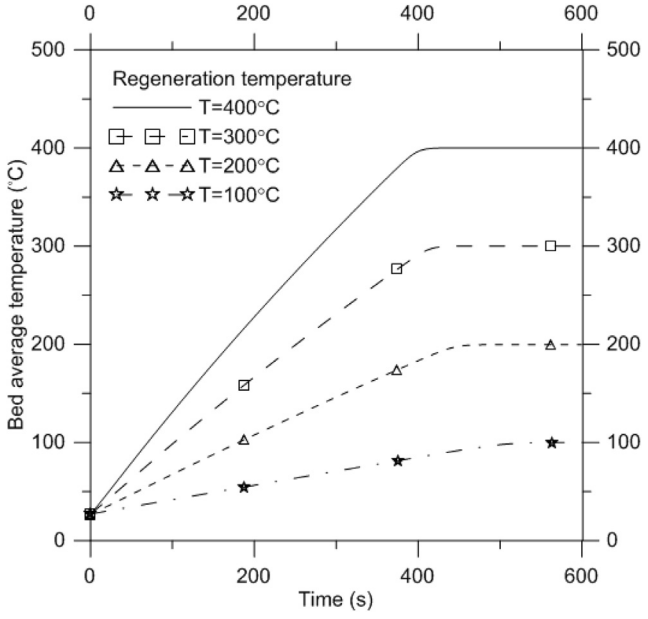

Fig. 10. Effect of the regeneration temperature on the bed average temperature.

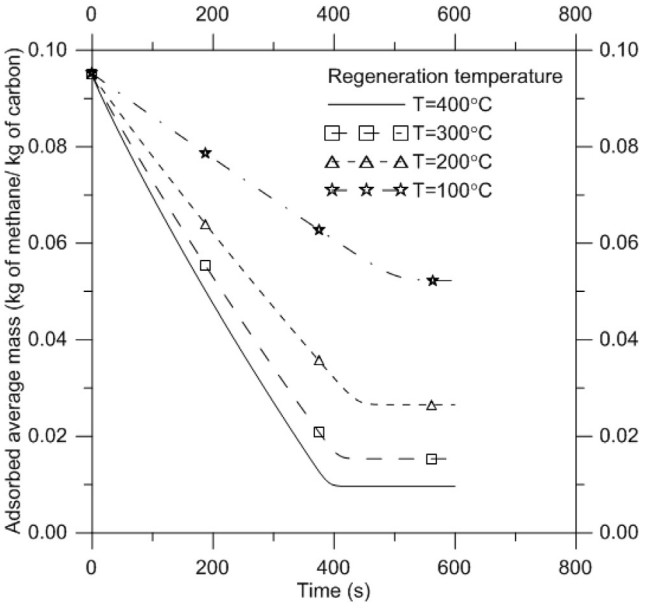

Fig. 11. Influence of the regeneration temperature in the adsorbed average mass.

For vehicles fueled with natural gas, the exhaust temperature can reach approximately 500 °C. Therefore, the exhaust gases can be used to pre-heat the regeneration gas in the column and provide the energy required by the desorption process. However, the maximum regeneration temperature obtained is limited by the available energy of the exhaust gases and the effectiveness of the heat exchanger employed. Another interesting fact is that temperature drops commonly found in the desorption process using the traditional storage tanks [5,6,8] are not observed for this configuration. This is mainly due to the opened adsorbent column used, where there is continuous flow of gas with high regeneration temperature, which ensures that the energy required for desorption is always available.

5.2. Influence of pressure drop to performance of the desorption process

In this section, we will investigate the effect of pressure difference between the inlet and outlet of column to the desorption of natural gas in activated carbon bed. Four pressure drops are considered: 400, 700, 1000, and 1300 Pa. Fig. 12 shows the effect of pressure drop on the average temperature of the adsorbent bed. It is observed that the progressive increase of the pressure drop imposed on the column implies a reduction of the time necessary for obtaining the maximum average temperature. The effect of pressure drop in the desorbed mass is shown Fig. 13. From this figure, it is possible to observe that increasing the pressure drop reduces the time required for the desorption process. It is also observed that the desorption time can vary between 250 and 600 s, depending on the applied pressure drop.

6. New proposed system to discharge process in ANG vessels

An efficient system for storing ANG needs to be able to compensate the temperature fluctuations observed in the adsorbent bed during the charge and discharge processes. In systems traditionally used for storing ANG, the adsorbent bed is connected to a source of gas through a single opening, and hence the gas can enter or exit the tank through this single opening. In these systems, the equilibrium between the internal and external pressure is reached instantaneously. When the equilibrium is reached, the gas flow is stagnant and heat conduction mode in the radial direction is the dominant heat transfer mechanism within the adsorbent bed. Due to the low effective thermal conductivity of the activated carbon bed and the thermal resistance imposed by the wall of the vessel, the system shows large temperature oscillations during the loading and unloading processes. From the numerical results obtained in this work in conjunction with an adsorbent column opened on both sides, it was observed that the temperature rise in the regeneration process increases the mass desorbed. It was also observed that increasing the pressure drop applied to the column reduces the desorption time. Therefore, we propose a new system configuration for performing the

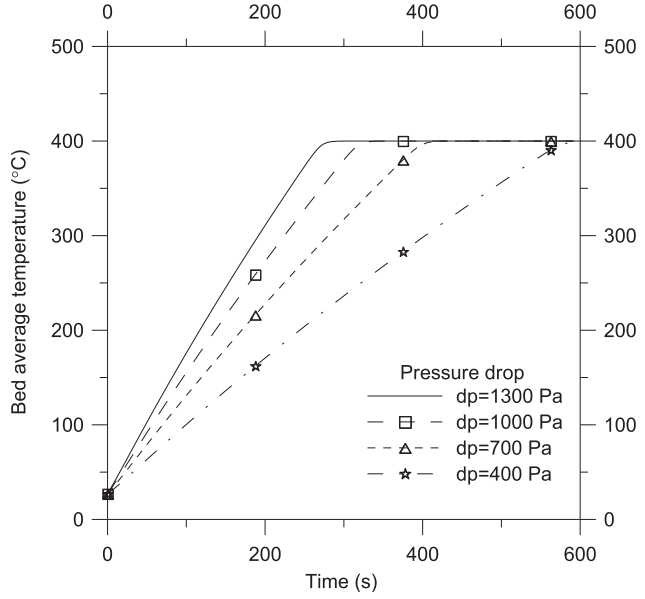

Fig. 12. Influence of applied pressure drop to the bed average temperature.

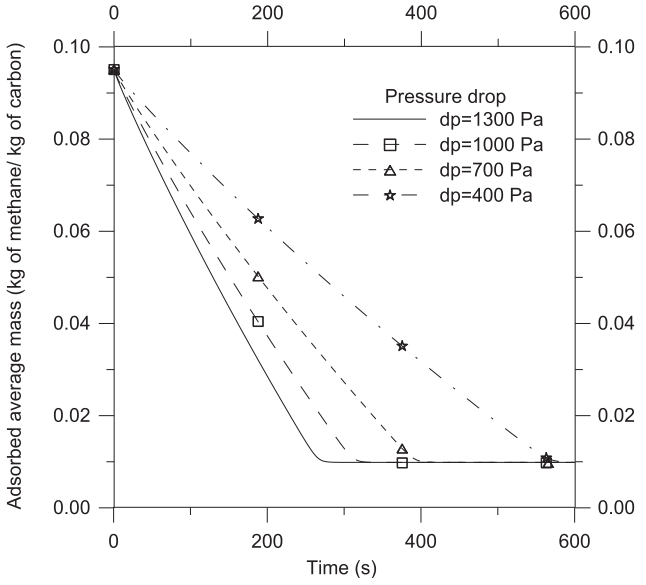

Fig. 13. Influence of applied pressure drop to the adsorbed average mass.

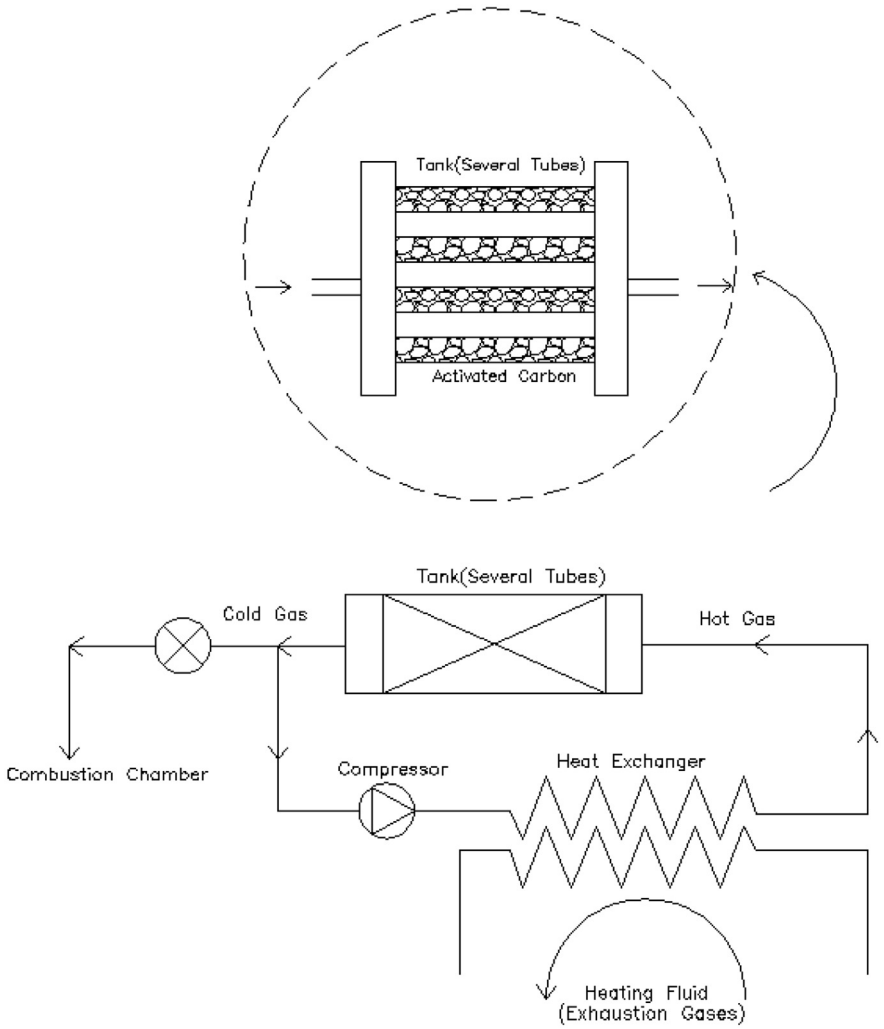

Fig. 14. New proposed system configuration.

discharging process that is able to take advantage of the previously mentioned results. The new tank configuration consists of several tubes packed with activated carbon and is shown in Fig. 14. The idea is to use forced convection between the adsorbent grains and the gas flow to improve the heat transfer into the bed. A fraction of natural gas that leaves the tank passes through an external heat exchanger, where the energy required for the desorption process is provided. We suggest the exhaust gases of the internal combustion engine as one of the heating fluids to be used in the heat exchanger. Finally, the heated gas is recirculated to the tank through a compressor to facilitate the unloading process in the adsorbent bed. Depending on the working conditions of the heat exchanger, the gas can enter into the tank overheated, increasing the desorbed mass. We can also optimize the compressor conditions to provide the pressure drop that minimize the discharge time of the tank. We can stress that the great advantage of the new proposed system is the use of forced convection inside the vessel in order to intensify the heat exchange into the system and reduce the harmful effects of heat of adsorption in ANG vessels. Besides providing satisfactory discharge times, the new suggested system does not use the accessories commonly used in traditional ANG vessels, such as fins and external heating jackets, which undermine the design versatility of ANG vessels.

7. Conclusions

This work presents a numerical investigation of the desorption dynamics of natural gas in a packed column with activated carbon. A computer code based on the finite-volume method was developed to solve the system of equations describing the dynamics of the regeneration process. The numerical results showed that the progressive increase of the inlet temperature of the gas in the column increases the desorbed mass, and therefore improves the performance of the regeneration process. The results also showed that the time required for the desorption is a function of the applied pressure drop in the column. Based on the obtained numerical results, a new tank configuration for performing the discharge process in ANG vessels has been suggested. It is expected that this new configuration will reduce the harmful effects of heat of adsorption during the process.

Acknowledgements

The authors thank the CNPq (The National Council for Scientific and Technological Development of Brazil) (305435/2012-4 and 305415/2012-3) and FUNCAP (The Foundation to Support the Scientific and Technological Development of Ceará-Brazil) (BP1-0067-00162.01.00/12) for their financial support.

References

[1] J.P.B. Mota, E. Saatdjian, D. Tondeur, A simulation model of a high-capacity methane adsorptive storage system, Adsorption 1 (1995) 17–27.
[2] D. Lozano-Castelló, J. Monge-Alcañiz, M.A. Casa-Lillo, D. Cazorla-Amorós, Advances in the study of methane storage in porous carbonaceus materials, Fuel 81 (2002) 1777–1803.
[3] J.P.B. Mota, I.A.A.C. Esteves, M. Rostam-Abadi, Dynamic modelling of an adsorption storage tank using a hybrid approach combining computational fluid dynamics and process simulation, Comput. Chem. Eng. 28 (2004) 2421–2431.
[4] F.N. Ridha, R.M. Yunus, M. Rashid, A.F. Ismail, Thermal analysis of adsorptive natural gas storages during dynamic charge phase at room temperature, Exp. Therm. Fluid Sci. 32 (2007) 14–22.
[5] F.N. Ridha, R.M. Yunus, M. Rashid, A.F. Ismail, Thermal transient behavior of an ANG storage during dynamic discharge phase at room temperature, Appl. Therm. Eng. 27 (2007) 55–62.
[6] K.J. Chang, O. Talu, Behavior and performance of adsorptive natural gas storage cylinders during discharge, Appl. Therm. Eng. 16 (1996) 359–374.
[7] L.L. Vasiliev, L.E. Kanonchik, D.A. Mishkinis, M.I. Rabetsky, Adsorbed natural gas storage and transportation vessels, Int. J. Therm. Sci. 39 (2000) 1047–1055.
[8] X.D. Yang, Q.R. Zheng, A.Z. Gu, X.S. Lu, Experimental studies of the performance of adsorbed natural gas storage system during discharge, Appl. Therm. Eng. 25 (2005) 591–601.
[9] J.C. Santos, F. Marcondes, J.M. Gurgel, Performance analysis of a new tank configuration applied to the natural gas storage systems by adsorption, Appl. Therm. Eng. 29 (2009) 2365–2372.
[10] D.M. Ruthven, Principles of Adsorption and Adsorption Processes, Wiley Interscience, New York, 1984.
[11] R.T. Yang, Gas Separation by Adsorption Processes, Butterworth, Boston, 1987.
[12] F.P. Incropera, D.P. DeWitt, Fundamentals of Heat and Mass Transfer, fourth ed., John Wiley & Sons, Inc, 1996.
[13] C.R. Maliska, Computational Fluid Mechanics and Heat Transfer, LTC, Rio de Janeiro, Brazil, 2004 (in Portuguese).
[14] S.V. Patankar, Numerical Heat Transfer and Fluid Flow, Hemisphere, New York, 1980.
[15] C.R. Maliska, A Solution Method Three-dimensional Parabolic Fluid Flow Problems in Nonorthogonal Coordinates (Ph. D. Thesis), University of Warterloo, Warterloo, Canada, 1981.
[16] G.D. Raithby, K.E. Torrance, Upstream-weight differencing schemes and their application to elliptic problems involving fluid flows, Comput. Fluids 2 (1974) 191–206.
[17] F. Marcondes, C.R. Maliska, Treatment of the inlet boundary conditions in natural convection flows in open-ended channels, Num. Heat Transf. Part B 35 (1999) 317–345.
[18] A. Malek, S. Farooq, Kinetics of hydrocarbon adsorption on activated carbon and silica gel, AIChE J. 43 (1997) 761–776.
[19] R.J. Remick, A.J. Tiller, Heat generation in natural gas adsorption systems, in: Gaseous Fuels for Transportation International Conference, Vancouver, Canada, 1996.
[20] R.D. Cess, Handbook of Heat Transfer, McGraw-Hill, New York, 1973.

Nomenclature

C_p: specific heat at constant pressure (J/kg K)
C_S: volumetric heat capacity of the adsorbent (J/m^3 K)
d_p: pellet diameter (m)
D_{ef}: effective mass diffusion coefficient (m^2/s)
q: concentration of the gas in adsorbent (kg/m^3)
$\overline{q}$: volumetric average concentration over pellet (kg/m^3)
u: interstitial velocity (m/s)
h: convection heat transfer coefficient (W/m^2 K)
ΔH: heat of adsorption (J/kg)
L: column length (m)
Nu: Nusselt number
p: gas pressure (Pa)
Pr: Prandtl number
r: pellet radial coordinate (m)
R: column radius (m)
Re: Reynolds number
R_g: ideal gas constant (J/kg K)
t: time (s)
T: temperature (K)
U_g: overall heat transfer coefficient (W/m^2 K)
x: axial coordinate in column (m)

Greek letters

ε: bed porosity
λ: thermal conductivity (W/m K)
ρ: specific mass (kg/m^3)

Subscripts

∞: relative to the ambient
0: relative to the initial condition
e: relative to the external surface
f: relative to the fluid phase
in: relative to the column inlet
p: relative to the pellet
S: relative to the solid phase
w: relative to the column wall

Superscripts

*: relative to the adsorption equilibrium